Available online at www.sciencedirect.com

ScienceDirect

Diamond & Related Materials 17 (2008) 1429 – 1433

DIAMOND AND RELATED MATERIALS

www.elsevier.com/locate/diamond

Piezo-actuated nanodiamond cantilever technology for high-speed applications

J. Kusterer [a,*], A. Lüker [b], P. Herfurth [a], Y. Men [a], W. Ebert [a], P. Kirby [b], M. O'Keefe [c], E. Kohn [a]

[a] Institute for Electron Devices and Circuits, University of Ulm, Germany
[b] School of Industrial & Manufacturing Science (SIMS), Cranfield University, United Kingdom
[c] Filtronic Compound Semiconductors Ltd., United Kingdom

Available online 15 February 2008

Abstract

Diamond cantilever actuators show high resonance frequencies but need also high actuation forces, pointing towards piezoelectric actuation by a PZT/diamond unimorph. In this study lead zirconate titanate ($Pb(Zr,Ti)O_3$, PZT) layers have been deposited onto nanocrystalline diamond films by sol–gel deposition, to realize high-speed MEMS actuators. The fabrication technology is based on self-aligned patterning and on optical lithography. A mechanical resonance frequency of 3.9 MHz has been obtained for 30 µm cantilever length dominated by the nanodiamond Young's modulus of approximately 1000 GPa.
© 2008 Elsevier B.V. All rights reserved.

Keywords: Nanodiamond; Piezoelectrics; PZT; MEMS

1. Introduction

Switches are an essential passive part of any electrical circuit. Used on-chip they need to be manufactured using microtechnology. However, in integrated circuits they are realized by switch transistors in many cases like for example in transmit/receive (TR) modules. But the conductivity limit in semiconductors will cause noticeable losses, even if heterostructure field effect transistors with high electron mobility channels are used. In some cases like phase shift antenna structures signal levels may be extremely low and transistor structures are difficult to integrate. An alternative concept is of course to use mechanical switches, which can be integrated into the semiconductor circuitry by direct monolithic integration or hybrid integration. Especially in the last case new materials may be implemented. However, although switching transistors have a high insertion loss, their signal delays may be in the ps-range, whereas most mechanical structures can only switch with µs-speed. In this investigation nanodiamond films have been investigated as base material for cantilever switches operating at high switching speeds up to the ns-range. As figure of merit, the mechanical resonance frequency was chosen, which should then reach into the MHz-range.

Nanocrystalline and ultrananocrystalline diamond films should provide a high resonance frequency of the basic cantilever, because of their high stiffness and low mass density [1]. In respect to the driving principles, which may be considered, these are the electrostatic, electrothermal, and piezoelectric drives [2]. Each one has specific advantages and drawbacks. The electrostatic drive is fast but needs high driving voltages in combination with stiff materials, which may then interfere with the signal path. The thermoelectric bi-metal driving principle can provide high bending moments, but switching may be limited by thermal time constants. The piezoelectric actuation can generate high bending moments at low voltages, if a material with high piezo-coefficients like lead zirconate titanate ($Pb(Zr,Ti)O_3$, PZT) can be used and if high driving fields can be generated without losses. It may therefore represent an optimum compromise, if the resonance of the diamond cantilever is not degraded by the mass densities and Young's moduli of the PZT piezoceramic and the associated contact layers. Previously, resonances up to 1 MHz had

* Corresponding author. University of Ulm, Institute for Electron Devices & Circuits, Albert-Einstein-Allee 45, 89081 Ulm, Germany. Tel.: +49 731 5026187; fax: +49 731 5026155.

E-mail address: joachim.kusterer@uni-ulm.de (J. Kusterer).

0925-9635/$ - see front matter © 2008 Elsevier B.V. All rights reserved.
doi:10.1016/j.diamond.2008.01.119

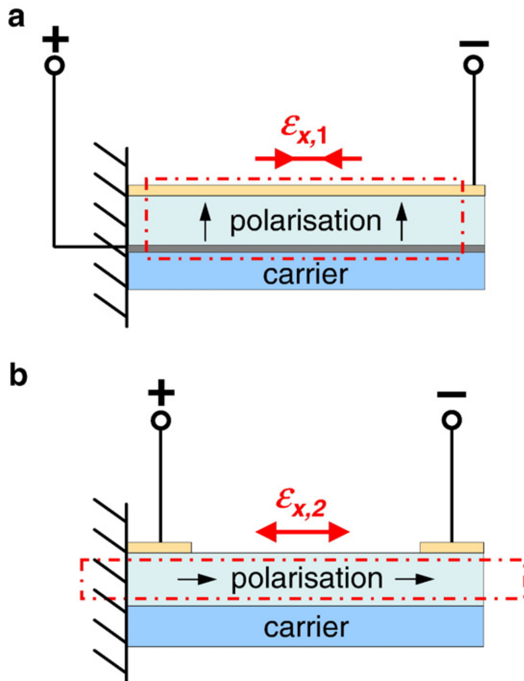

Fig. 1. a: Longitudinal mode of a piezoelectric unimorph. An applied electrical field induces an elongation of the piezoceramic and leads thus to downward bending of the cantilever structure. b: Transversal mode of a piezoelectric unimorph. An applied electrical field induces a contraction of the piezoceramic and thus leads to upward bending of the cantilever structure.

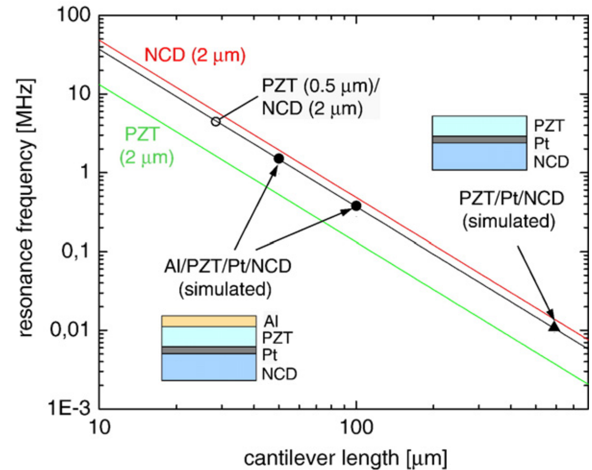

Fig. 2. Calculated resonance frequencies (Eq. (1)) of single layer cantilevers of 2.0 µm PZT and NCD and multilayer stacks of 0.5 µm PZT/2.0 µm NCD. Also plotted are three points for the simulation of three complete Al/PZT/Pt/NCD stacks of 50, 100, and 590 µm length with thicknesses as mentioned in the text; for Young's moduli see Table 1.

been observed with UNCD/PZT unimorphs using reactive sputter deposition of PZT [3].

In this investigation a diamond/PZT unimorph has been investigated, using PZT deposited by a sol–gel technique as described previously [4]. This unimorph structure was then analysed theoretically, manufactured using a self-aligned patterning technique and dynamically tested.

2. Design

2.1. Modes of operation

Typically, two different modes can be used in the design of a piezoelectrically actuated unimorph. This is firstly the longitudinal mode (d_{33}-mode; Fig. 1a), where the polarisation of the piezoceramic is laterally developed in the deposited film, which is in direction of the cantilever length. Both associated electrodes may be placed on top of the film. An applied electrical field stimulates elongation or contraction ($\varepsilon_{x,1}$) depending on the polarization of the stimulating bias. Normally contraction is limited by the materials stability and therefore very limited in use. Elongation results in downward bending of the actuator, if the piezoelectric film is deposited on top of the beam.

In the transversal mode (d_{31}-mode; Fig. 1b) piezoelectrically induced stress is in the vertical direction and the film is either vertically stretched and contracted ($\varepsilon_{x,2}$), with stretching being the more stable regime. In this case the beam is lifted up.

In general, the longitudinal piezoelectric strain coefficients of PZT (d_{33}) are approximately twice as large as the longitudinal ones (d_{31}) and can reach values up to 630 pm/V [5]; therefore this mode of operation is usually preferred. In this study, however, the transversal mode is used in order to make use of a self-aligned fabrication technology.

2.1.1. Resonance behaviour

Piezoelectric actuators are mostly used in switches [6] or mechanical resonators [2,7]. In both applications the mechanical resonance frequency represents the first limit in the speed of deflection. To the first order, the resonance frequency f_r of a bi-layer system like a piezoelectric PZT/NCD unimorph is given by [8]:

$$f_r = \frac{1.875^2 t}{4\pi L^2}\sqrt{\frac{E_{PZT}}{3\rho_{PZT}}}\left[\frac{A^2B^4 + 2A(2B + 3B^2 + 2B^3) + 1}{(1 + BC)(AB + 1)(1 + B)^2}\right]^{1/2} \quad (1)$$

where E_{PZT} and ρ_{PZT} denote the Young's moduli and density of mass of the piezoceramic, t and L are the total thickness and length of the cantilever beam, $A = E_{NCD}/E_{PZT}$ are the ratio of the Young's moduli of NCD and PZT, and $B = t_{NCD}/t_{PZT}$ the ratio of the layer thicknesses of NCD and PZT, respectively. A fixed thickness ratio of the NCD/PZT results in a reciprocal square law relationship with cantilever length (see also slope of graphs in Fig. 2).

Table 1
Materials properties for PZT and various base materials

Material	NCD	Silicon	SiC	Al	Pt	PZT
Young's modulus (YM) [GPa]	800–1000	160	400	70	168	80
Density of mass (ρ_m) [g/cm^3]	3.52	2.33	3.21	2.70	21.09	7.50
$\sqrt{YM/\rho_m}$ [10^3 m/s]	16.9	8.4	11.2	5.1	2.8	3.3

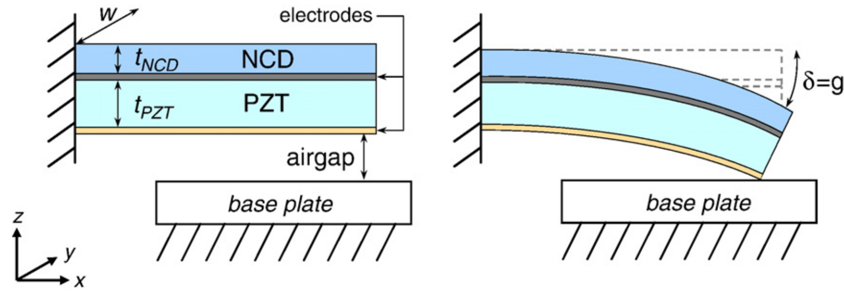

Fig. 3. Operation of PZT/NCD unimorph. The applied electrical load induces cantilever bending until an initial airgap (g) towards a base plate is closed ($\delta = g$); for even higher loads a force (F) onto the base plate is generated.

It is seen, that high resonance frequencies are expected for thick and short beams on the one hand, and for stiff materials with low density of mass on the other hand. However, in these cases also high deflection forces are needed. Diamond is best suited as seen from Table 1, and needs now to be combined with a deflection mechanism of high force, which had already been mentioned in the introduction and is the piezoelectric PZT/diamond unimorph.

Fig. 2 illustrates the resonance frequencies, which can be obtained with these various base materials assuming a beam thickness of 2.0 µm as function of beam length using finite element analysis (FEA). The MHz-range is reached for diamond cantilevers of approximately 60 µm length, whereas in Si this length would need to be below 40 µm.

If diamond is employed as base material, the fully operational actuator would also need to contain an interfacial adhesion layer between the diamond and PZT ceramic layer, which is a 100 nm Pt film also serving as the bottom electrode, a 0.5 µm thick PZT film and a top electrode, which has been 50 nm Al in our case. Fig. 2 shows the resonances corresponding to each material and the shift due to the additional masses added in the multilayer stack for different cantilever lengths. It is observed, that the PZT film degrades the resonance frequency by only 15%. Adding the metallization layer will not cause any noticeable additional degradation.

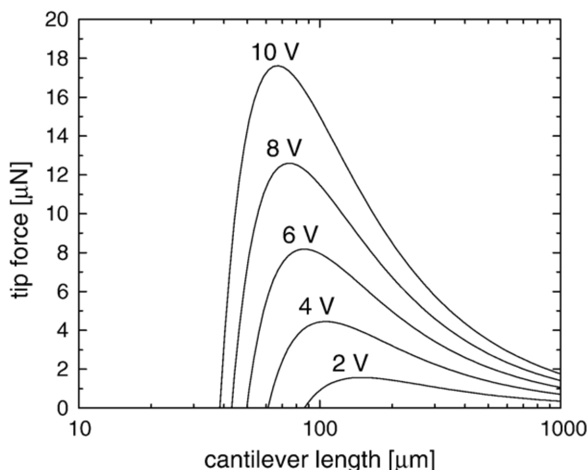

Fig. 4. Calculated tip contact force of PZT/NCD unimorph depending on beam length for different applied voltages (using Eqs. (1) and (2)).

2.1.2. Cantilever deflection

When applying an electrical field across the piezoelectric film, the strain generated between the piezoelectric film and the carrier substrate leads to a bending moment, which can either cause a deflection of the beam or can generate a force onto a base plate after the air gap is closed (see Fig. 3).

Data of the deflection and force respectively may be obtained from Eqs. (2) and (3) [8]:

$$\delta = \frac{3L^2}{2t} \cdot \frac{2AB(1+B)^2}{A^2B^4 + 2A(2B + 3B^2 + 2B^3) + 1} \cdot d_{31} \frac{V}{t_{PZT}} \tag{2}$$

$$F = \frac{3wt^2 E_{PZT}}{8L} \cdot \frac{2AB}{(AB+1)(1+B)} \cdot d_{31} \frac{V}{t_{PZT}} \tag{3}$$

where L, t, w are the cantilever length, entire thickness ($t_{PZT} + t_{NCD}$), and width, d_{31} the transversal piezoelectric coefficient, V the applied voltage, E_{PZT} the Young's modulus of the piezoelectric layer, $A = E_{NCD}/E_{PZT}$ the ratio of the Young's moduli of diamond and PZT, and $B = t_{NCD}/t_{PZT}$ the ratio of the layer thicknesses, respectively.

As actuator in a switch application, in the quiescent condition (without external electrical field) the switch is typically in the open condition and the cantilever separated from the base plate contact by an airgap. A force onto the base is therefore generated only after the cantilever has touched the base plate and the deflection is equal to the airgap. The diagram in Fig. 4 shows a calculation of the generated force for a 0.2 µm airgap as

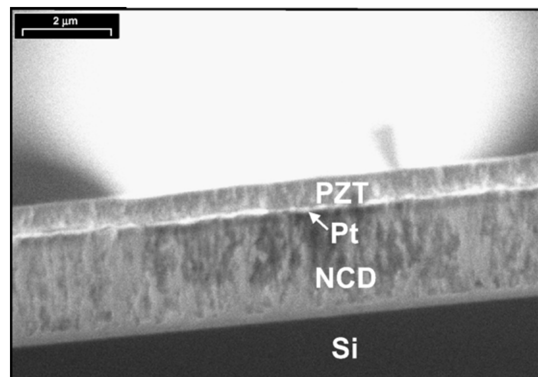

Fig. 5. Cross section SEM view of a sol–gel derived PZT film on NCD including Pt adhesion layer. The film was post-annealed at 570 °C and is crystallized in the perovskite phase [4].

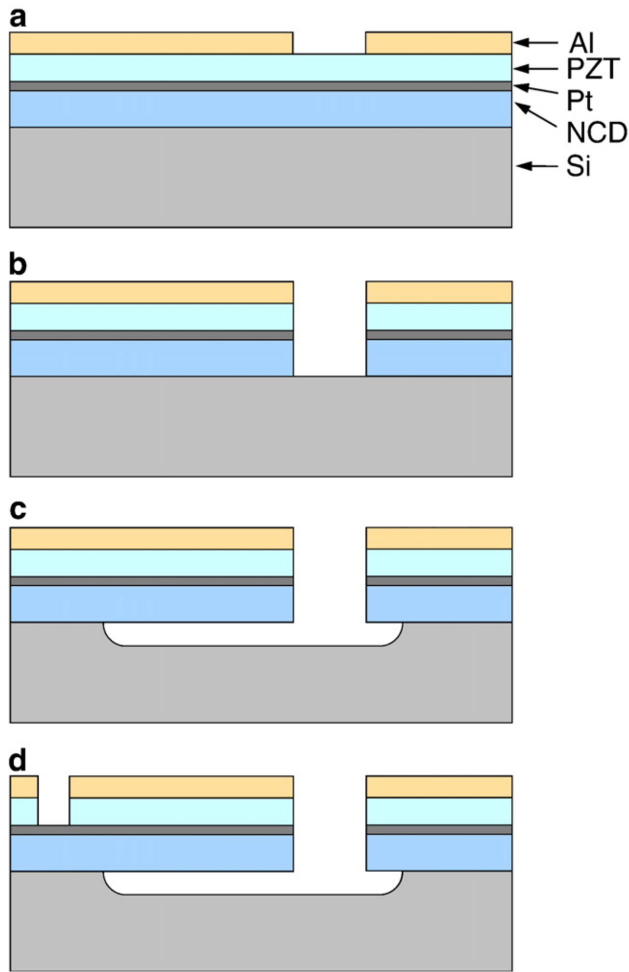

Fig. 6. Process flow of unimorph PZT/NCD piezoactuator fabrication.

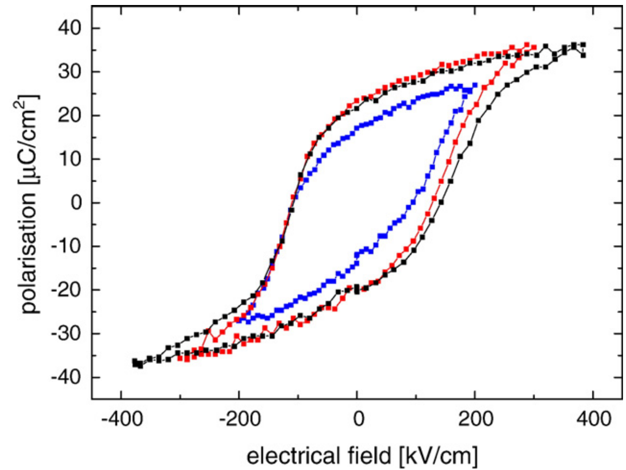

Fig. 8. Measured hysteresis curve for polarisation of sol–gel PZT on NCD.

function of applied voltage (cantilever data: 0.5 μm PZT on 2.0 μm NCD, width = 6 μm). It can be observed that the force increases for shorter cantilevers up to a maximum; for very short beams, where the maximum applicable field (~240 kV/cm; determined by device failure) results in a voltage, which is to low to close the airgap, no contact force can be generated.

2.2. Technology

The starting material for the cantilever actuator structure was a 2.0 μm thick NCD film with a grain size of approx 50 nm deposited onto a <100>-oriented Si-substrate. The film was grown by MWPECVD with high re-nucleation rate to obtain a stress balanced film (3D NCD; [9]). Usually the following step is the deposition of a metallic bottom electrode. This layer serves also as oxygen diffusion barrier during PZT deposition and the following post-annealing step and as adhesion layer to accommodate the high bending moments required by the high diamond stiffness. PZT can be deposited by MOCVD [10], pulsed laser deposition [11], sputter deposition [3], ECR-PECVD [12], atomic layer deposition [13], or sol–gel spin-on [7,14]. Most of these methods need a post-annealing step for dipole orientation in the perovskite structure in the range of 550–650 °C. In this work a sol–gel process was used for PZT deposition. The adhesion layer and bottom electrode was PVD platinum. The sol–gel PZT was deposited using a spin-coater and post-annealed at 570 °C in ambient atmosphere [4]. This method and material combination benefits from homogenous and large area deposition at low thermal budget. A cross sectional view of this material system is illustrated with Fig. 5.

After realization of the Si/NCD/Pt/PZT material stack the Al top electrode is deposited by evaporation and patterned by lithography to define the cantilever geometry. This pattern serves then as hard mask for the anisotropic dry etching of the PZT/Pt/NCD stack in different atmospheres of Ar and Ar/O_2, respectively, and the undercut isotropic plasma etching in CF_4/O_2 of the Si-substrate to release the cantilever beam. It

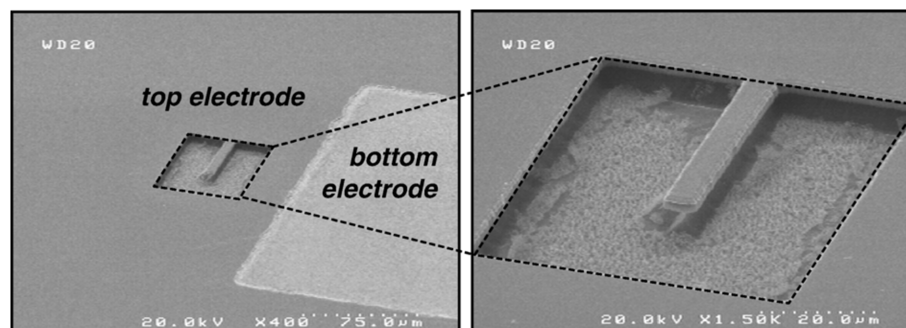

Fig. 7. Fabricated cantilever actuator with 50 μm length.

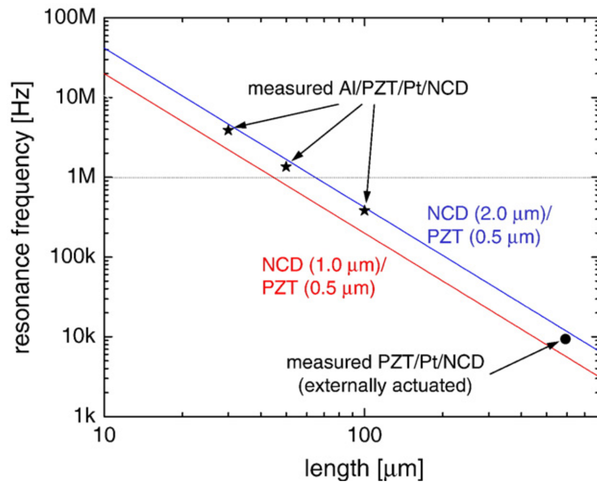

Fig. 9. Measured resonance frequencies of piezoactuators having different cantilever lengths. The 30 µm and 50 µm beams possess resonance frequencies in the MHz-range as simulated.

is therefore self-aligned and the top electrode covers the entire cantilever surface to obtain a uniform electrical field across the piezoceramic. In a last step the bottom Pt electrode is contacted through a wet chemically etched window. The entire fabrication process is sketched with Fig. 6; Fig. 7 shows SEM micrographs of a processed 50 µm cantilever.

3. Results

Fig. 8 shows the hysteresis curve for polarisation obtained after deposition of PZT. It can be observed that PZT indeed shows piezoelectric behaviour and is well suited for actuator fabrication.

Additionally, to optimise piezoelectric properties and prepare for operation the PZT film was poled at 120 °C under an electrical field of 200 kV/cm for 60 min. After this step DC leakage current density was determined at an electrical field of 50 kV/cm to approximately $2 \cdot 10^{-8}$ A/cm^2, which corresponds to a resistivity in the TeraΩcm regime.

To determine the mechanical resonance, the beams were stimulated by a sinusoidal signal and the resonance oscillation identified visually. To avoid inverse polarity across the piezoceramic, a DC offset of half of the peak voltage was added. Cantilevers of 30, 50, 100 and 590 µm lengths have been stimulated.

Measured data are compiled in Fig. 9, where they are compared with their calculated performance using Eq. (1) for two NCD film thicknesses of 2.0 and 1.0 µm. This represents the experimental spread of thickness of the wafer used. It is seen, that the measured data follow indeed the theoretical prediction. Accordingly, resonances in the MHz-range are measured for the two shortest lengths of 50 µm and 30 µm with the highest resonance of 3.9 MHz for the 30 µm cantilever beam.

4. Conclusions

Nanodiamond piezoelectric cantilever actuators were realized using a sol–gel spin-on PZT piezoelectric ceramic film to demonstrate MHz mechanical resonance performance. Indeed cantilevers with 30 µm length exhibited 3.9 MHz resonance frequency, identified visually when being stimulated by a sinusoidal signal. The result is in full agreement with calculated and simulated data. Diamond piezoelectric actuators may therefore be considered a realistic concept to realize high-speed resonators and switches. In comparison to the thermoelectric and electrostatic actuation this concept needs only a small actuation voltage without static losses, it does not suffer from snap-in when used in switches, and pull back when opening the switch may be accelerated by reversing the driving potential.

Acknowledgements

The authors are grateful to Ulrich Heinle from Microgan GmbH for many fruitful discussions and help in respect of the applied technology. Also, special thanks are to Silvana Corkovic from Cranfield University for helpful discussions in respect of the PZT materials properties. Funding was in part provided by the German Research Association (DFG).

References

[1] O. Auciello, J. Birrell, J.A. Carlisle, J.E. Gerbi, X. Xiao, B. Peng, H.D. Espinosa, Journal of Physics: Condensed Matter 16 (2004) R539–R552.
[2] J. Kusterer, P. Schmid, E. Kohn, New Diamond and Frontier Carbon Technology 16 (2006) 295.
[3] S. Srinivasan, J. Hiller, B. Kabius, O. Auciello, Applied Physics Letters 90 (2007) 134101.
[4] J. Kusterer, A. Lüker, W. Ebert, Q. Zhang, P. Kirby, E. Kohn, "Pb(Zr,Ti)O_3 on CVD diamond: A new material system for MEMS actuators", Presented at the Diamondconference 2006, 17th European Conference on Diamond, Diamond-Like Materials, Carbon Nanotubes, Nitrides & Silicon Carbide, 3–8 September, 2006, 2006 Estoril, Portugal, [5.6.08].
[5] APC International Ltd., "Piezoelectric Ceramics: Principles and Applications", Mackeyville, PA, USA, 2002 ISBN 0-9718744-0.
[6] H.W. Jiang, P.B. Kirby, Q. Zhang, Proceedings - SPIE The International Society For Optical Engineering 4979 (2002) 165.
[7] F.F.C. Duval, R.A. Dorey, R.W. Wright, Z. Huang, R.W. Whatmore, Integrated Ferroelectrics, 63 (2004) 27.
[8] Q.-M. Wang, Q. Zhang, B. Xu, R. Liu, L.E. Cross, Journal of Applied Physics. 86 (1999) 3352.
[9] T. Zimmermann, K. Janischowsky, A. Denisenko, F.J. Hernández Guillén, M. Kubovic, D.M. Gruen, E. Kohn, Diamond and Related Materials 15 (2006) 203.
[10] J.S. Zhao, D.-Y. Park, M.J. Seo, C.S. Hwang, Y.K. Han, C.H. Yang, K.Y. Oh, Journal of. Electronic Chemical Society 151 (2004) C283.
[11] Q. Wan, N. Zhang, L. Wang, Q. Shen, C. Lin, Thin Solid Films 415 (2002) 64.
[12] S.-O. Chung, H.-C. Lee, W.-J. Lee, Japanese Journal of Applied Physics 39 (2000) 1203.
[13] Takayuki Watanabe, Susanne Hoffmann-Eifert, Frank Peter, Shaobo Mi, Chunlin Jia, Cheol Seong Hwang, Rainer Waser, Journal of The Electrochemical Society 154 (2007) G262.
[14] J. Zeng, L. Wang, J. Gao, Z. Song, X. Zhu, C. Lin, L. Hou, E. Liu, J. Crystal Growth 197 (1999) 874.